COMPARISON OF FLOW FIELDS OF A PURE FLUID AND A ZEOTROPIC MIXTURE FOR CONDENSATION IN A SHELL-AND-TUBE CONDENSER

T. Karlsson, Ph.D, Heat and Power Technology, Department of Chemical Engineering and Environmental Science, Chalmers University of Technology, Gothenburg, Sweden, Alpha Solutions AB, Gothenburg, Sweden, Tord.Karlsson@alphasolutions.se

ABSTRACT

Condensation of a pure refrigerant and a zeotropic refrigerant mixture in a shell-and-tube condenser is investigated in an advanced calculation model based on a developed condensation routine coupled to a commercial CFD program. The aim of the investigation is to make a three-dimensional calculation model for mixture condensation, and to see if previous results from 2D calculations also can be seen in 3D calculations, namely a significant difference between the flow fields of a pure fluid and a mixture. The calculation results presented here show the same tendencies as 2D calculations in the earlier work. The flow field of the mixture is much more complex than that of the pure refrigerant. Large vortexes arise, starting at the top of the shell, going down along the shell and into the tube bundle from below. Vapour is therefore mainly fed from below, causing a counterflow between vapour and condensate. A well-mixed condensate, which here is an unfavourable situation, results in a performance 30 % lower compared to the case where the condensate phase is unmixed. The latter is normally considered to be the inferior case.

Keywords: ***condensation, zeotropic, mixture, flow field, CFD, shell-and-tube.***

1 INTRUDUCTION

1.1 General Background

Shell-and-tube condensers with condensation on the shell-side are widely used in large heat pumps. This typically means that the condensing medium, in this case a refrigerant, is fed to the top of a shell-and tube heat exchanger, and then while flowing around the tubes in the tube bank the vapour condenses, leaving its latent heat to the cooling medium flowing inside the tubes. The condensate is driven by gravity towards the bottom of the shell, where it leaves the condenser as a saturated or subcooled liquid.

The heat transfer in a shell-and-tube condenser is complicated to predict. Factors such as the complex geometry of the tube bank, effect of the tube surface geometry, vapour shear effects and condensate inundation from the tubes above all have an effect on heat transfer. Many studies have been performed to better understand, and be able to predict, heat transfer for condensation on the outside of horizontal tubes. The reference work for most studies is the theoretical model for a single, smooth, horizontal tube, developed by Nusselt (1916).

Lately, substantial work has been focused on the behaviour of zeotropic mixtures. One reason for this is the Montreal Protocol which regulates the use of chlorofluorocarbons (CFCs) and hydrochlorofluorocarbons (HCFCs) in the refrigeration industry (UN 1989). This makes hydrofluorocarbons (HFCs), or mixtures of them, obvious substitutes. Two or more HFCs can be mixed to obtain desired thermophysical properties, still with a low environmental impact. For many mixtures a gliding temperature difference (GTD) arises, which means that there is a risk of too small temperature difference between the heat sink and the condensing refrigerant. The result can be an undesired low rate of heat transfer in part of

NOMENCLATURE

A	heat transfer area [m^2]	δ	thickness [m]
c_p	specific heat [J $kg^{-1}K^{-1}$]	Γ	mass flow rate [kg $m^{-1}s^{-1}$]
D	diffusivity [m^2s^{-1}]	λ	thermal conductivity [W $m^{-1}K^{-1}$]
d_{eq}	equivalent diameter [m]	μ	dynamic viscosity [Pa s]
F	momentum source [N]	ρ	density [kg m^{-3}]
g	gravitational acceleration [m s^{-2}]	τ	stress tensor [kg $m^{-1}s^{-2}$]
h	heat transfer coefficient [W $m^{-2}K^{-1}$]		
h_{fg}	specific heat of vaporization [J kg^{-1}]	*Subscripts*	
J	mass flux [kg $m^{-2}s^{-1}$]	β	at angle β on a tube
M	mass flux [kg s^{-1}]	*c*	cooling medium
M	molar mass [g/mol]	*cc*	cooling of condensate
p	pressure [Pa]	*cond*	condensate
Q	heat flux [W]	*cond*	newly formed condensate
S	mass source [kg $m^{-3}s^{-1}$]	*eq*	at equilibrium
R	fouling resistance [m^2K W^{-1}]	*I*	interface
T	temperature [K]	*i*	component index
t	time [s]	*i*	inside
u	velocity [m s^{-1}]	*i'*	coordinate direction
U	overall heat transfer coefficient [W $m^{-2}K^{-1}$]	*inflow*	flowing in from tube above
V	molecular diffusion volume	*j'*	coordinate direction
x	coordinate [m]	*l*	liquid film
x	liquid mass fraction [-]	*m*	mixture
y	vapour mass fraction [-]	*o*	outside
		sat	saturated conditions
Greek symbols		*sat*-1	saturated conditions on tube above
β	angle [rad]	*w*	tube wall

the equipment, and for condensation the worst case can be accumulation of the more volatile component due to a too low dew point. This is becoming more important since there is a trend towards lower temperature driving forces in systems today.

Studies of mixture condensation outside a horizontal tube bundle have shown a decrease in heat transfer coefficient for mixtures compared to pure components. Honda et al. (1999, 2002) tested different tube geometries in a tube bundle, and found a considerably lower heat transfer coefficient for a mixture than for pure R123 and R134a, for all geometries. They concluded that the difference was greater for lower mass velocities and lower temperature differences, and that the reason is the diffusive transport resistance in the vapour film closest to the gas-liquid interface. Belghazi et al. (2001, 2003) recorded a decrease of 30-50% in heat transfer coefficient for the mixture R23/R134a with the same explanation. Jung et al. (2003a, 2003b) measured heat transfer coefficients for the ternary mixture R407C on a single smooth, horizontal tube, and found up to 50% lower heat transfer coefficients than for R22. Gabrielii and Vamling (1997) studied R22 and three different mixtures experimentally in a full-scale condenser, and found a decrease of up to 70% in heat transfer for the mixtures. Sajjan et al. (2004) and Karlsson and Vamling (2004a) studied the condensate flow theoretically and concluded that, besides the diffusive resistance in the vapour film closest to the interface, mass transfer resistance in the condensate is also an important factor for the decrease in heat transfer for mixtures.

One thing has been overlooked in all investigations mentioned above, namely the effect of the flow field in a condenser. All investigations have been based on an assumption of a nicely vertical flow field around the tube bank. Only in the measurements on a full-scale condenser carried out by Gabrielii and

Vamling (1997) the vapour flows freely around the tube bank. However, the theoretical investigations connected to the measurements are again idealized to a strictly vertical flow field. The main reason for this simplification is the complexity of the problem if the flow field is to be solved together with multi-component condensation. There is, however, a tool that can solve problems as complex as this, and an attempt to use it on mixture condensation was done by Karlsson and Vamling (2004b). They carried out two dimensional calculations for a small shell-and-tube condenser with commercial CFD software, where CFD stands for Computational fluid dynamics. The conclusions were that the flow field of a mixture is different than that of a pure fluid, and that a change in flow field for the mixture, i.e. by a change in inlet design, can have a great influence on the total heat flux in the condenser.

1.2 Computational Fluid Dynamics

Computational fluid dynamics (CFD) is generally a computer program that solves fluid dynamics problems. Today it is however capable of doing much more than that. It can solve all kinds of problems including transport phenomena for an arbitrary geometry. Thanks to the rapidly enhanced computational power of standard personal computers, CFD has grown into being a versatile and usable tool in research and development.

During the last couple of years the solvers have improved a lot. They are now relatively stable and have become much faster than they used to be. Most CFD software utilize a finite element-based control volume method in the solver, which is a powerful solution method. More details on models and solvers can be found in the manuals and on the websites of each software producer. In this work a commercial CFD program called Fluent is used.

A review of the available literature shows that little work in the field of heat exchange has used commercial CFD programs. Perrotin and Clodic (2004) used CFD to calculate flow field and heat transfer in a heat exchanger and Liu et al. (2004) used CFD when analyzing wall condensation in a chamber. The list of CFD work could be made long, but no work using CFD for investigating condensation on tube banks could be found in the recently published literature, except for the previously mentioned work by Karlsson and Vamling (2004b).

To solve the problem of phase change in a condenser is still difficult, even for a modern CFD program, since the liquid and the vapour flows have different flow fields, and the liquid flow is very complex to describe. In order to solve the liquid film flow on the tubes and the drops of liquid between tubes in a shell-and-tube condenser, a very high resolution of the computational mesh is required, which would demand a great computational effort. In addition, other problems arise regarding stability and obtaining convergence in the solution, which still makes the tool insufficient. To be useful for such a complex problem, simplifications are necessary.

2 AIM

The aim of this work is to build an advanced three-dimensional condenser model in a commercial CFD program and to theoretically investigate the flow fields of pure R22 and the binary mixture R32/R134a. With the calculation model the difference in behaviour between a pure fluid and a zeotropic mixture will be investigated. It is not only important to investigate the heat transfer coefficient on the first tube or the progress in a perfect, rectangular tube bundle, which has been done by many researchers experimentally, as was mentioned in the introduction, but it is also important to see what effects the gliding temperature difference and the mass transfer resistances can have on the flow field and on the condensation process in a geometry similar to that of real condensers and vice versa. Previously two dimensional calculations were carried out by Karlsson and Vamling (2004b), and this work is a first attempt to extend the analysis into three dimensions.

3 THEORY AND CALCULATIONS

The good thing about using a commercial CFD program is that all basic flow equations are already defined, and an efficient solver is only a click away. However, in order to use the full potential of the program, subroutines written in a standard programming language can be incorporated. The subroutines developed for this work will be described below together with a description of the condenser used in the investigations.

3.1 General Considerations

The condenser is the same as was described by Karlsson and Vamling (2004b), where a two-dimensional analysis was carried out. Here the same condenser has been extruded into three dimensions. The condenser geometry can be seen in Fig. 1. It is a small shell-and-tube condenser, only 0.7 m long and with 100 tubes. The tubes are of low-finned type with a diameter of 19 mm, the horizontal tube pitch is 24 mm and the vertical tube pitch is 21 mm. The condenser dimensions are small in order to save calculation time. In order to make the calculation geometry even smaller, a symmetry plane is used, seen to the right in Fig. 1.

The condenser is two-pass on the tube side. Water is fed to the tubes in the lower tube pass at 294 K. The flow rate is adjusted so that the temperature is 298 K when the water leaves the condenser from the upper tube pass. Two different refrigerants are tested; pure R22 and a binary mixture of R134a and R32. The binary mixture is the commercially available R407C with R125 replaced by additional amounts of R32. The binary mixture is similar in properties to R407C and it is used only because a binary mixture speeds up the calculations compared to a ternary mixture. The gliding temperature difference (GTD) of both mixtures is around 5.5 K. The refrigerant enters through the inlet at the top of the condenser as saturated vapour at 310 K for the mixture and at 308 K for pure R22. The temperature of the mixture is slightly higher due to the GTD.

In order to avoid problems involved with solving the liquid phase rigorously, a simplified approach is taken. The liquid flow is not solved as a separate phase in the calculations. Instead a one-phase vapour system is solved, and the influence of the liquid on the vapour flow is included as source terms in the transport equations. The condensation process is simulated as negative source terms around all tubes, removing vapour from the system. This means that the system has a vapour inlet (at the top), but no outlet. All vapour is removed by source terms around the tubes.

All calculations regarding rate of condensation, heat flux and interaction between the vapour and liquid phases are solved in separately written subroutines, called by the main CFD program every iteration. In this way a solution can be obtained with a reasonable computational effort. More details will be given below.

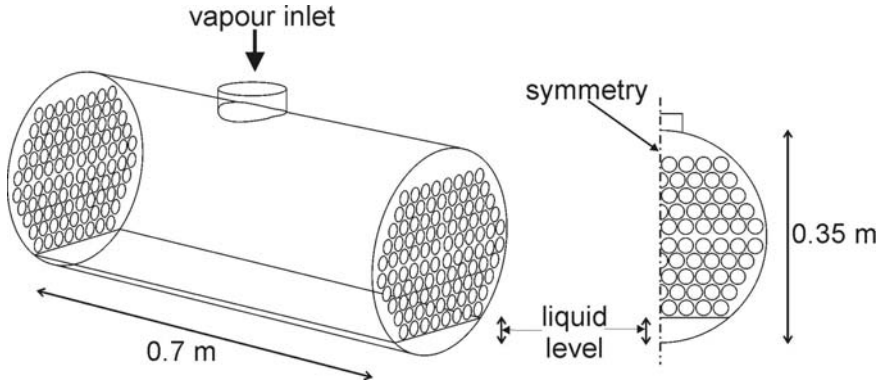

Fig. 1. Condenser geometry used in the calculations. The symmetry plane can bee seen to the right.

3.2 Set-up and Solution of the Vapour Flow Field

The first step in setting up a problem with a CFD program is to define the geometry, here described by Fig. 1. This is typically done in a CAD environment. Next the geometry is meshed, which means that the geometry is divided into a great number of small volumes, usually tetrahedrons, hexahedrons or prisms. These smaller volumes are used when all equations are discretized by the solver.

Next step is to define the physical properties of the problem and to set all boundary conditions. A number of standard properties and boundary conditions are available in the CFD program, but if the desired property or boundary condition is not available, it is possible to write subroutines separately in a standard programming language. These subroutines are coupled to the CFD program, and are then available for use. This makes the CFD program flexible.

There are a number of basic equations that all CFD programs are based upon. The first one is the mass conservation equation:

$$\frac{\partial \rho}{\partial t} + \sum_{i'} \frac{\partial}{\partial x_{i'}} \left(\rho u_{i'} \right) = S \tag{1}$$

and it is solved together with the momentum conservation equations:

$$\frac{\partial}{\partial t} \left(\rho u_{i'} \right) + \sum_{j'} \frac{\partial}{\partial x_{j'}} \left(\rho u_{j'} u_{i'} \right) = -\frac{\partial p}{\partial x_{i'}} + \sum_{j'} \frac{\partial \tau_{j'i'}}{\partial x_{j'}} + \rho g_{i'} + F_{i'} \tag{2}$$

In the above equations *i'* and *j'* are coordinate directions, and there is one equation (2) for each coordinate direction in the problem. *S* in equation (1) is a mass source term and $F_{i'}$ in equation (2) is a momentum source term. If the problem involves more than one species, equations for conservation of each species must be solved together with equations (1) and (2):

$$\frac{\partial}{\partial t} \left(\rho y_i \right) + \sum_{i'} \frac{\partial}{\partial x_{i'}} \left(\rho u_{i'} y_i \right) = \sum_{i'} \frac{\partial}{\partial x_{i'}} \left(J_{i,i'} \right) + S_i \tag{3}$$

For a mixture of *n* components, *n*-1 species conservation equations must be solved. In equation (3) y_i is mass fraction of component *i*, S_i is a mass source term for species *i*, and $J_{i,i'}$ is the diffusive transport expressed as

$$J_{i,i'} = -\rho D_{i,m} \frac{\partial y_i}{\partial x_{i'}} \tag{4}$$

$D_{i,m}$ is the diffusion coefficient for component *i* in the mixture. In this work it is calculated according to Fuller et al. (1966):

$$D_{12} = C T^{1.75} \frac{\sqrt{\left\{ \left(M_1 + M_2 \right) / M_1 M_2 \right\}}}{P \left\{ \sqrt[3]{V_1} + \sqrt[3]{V_2} \right\}^2} \tag{5}$$

where D_{12} is the binary diffusion coefficient, *C* is a constant, *M* is the molar mass and *V* is the molecular diffusion volumes, and they are calculated by summing atomic contributions from a table, see Fuller et al. (1969).

3.3 Influence of Condensate Flow on the Vapour Flow Field

The condensate phase is not solved explicitly, but the influence of the condensate on the vapour is included as much as possible. First of all, the condensate has a downward flowing motion on all tubes since it is drained by gravity. Therefore all tube walls are modelled as moving walls. The velocity de-

pends on the angle around the tube, with zero velocity on top and bottom. It depends on the angle β, relative to the horizontal plane, according to Bird et al. (2001):

$$u_\beta = \frac{\rho g \delta^2 \cos\beta}{2\mu} \tag{6}$$

where δ is the condensate thickness, calculated as:

$$\delta = \sqrt[3]{\frac{3\mu\Gamma}{\rho^2 g \cos\beta}} \tag{7}$$

Here Γ is the mass flow per metre of tube, which is adjusted for the area enhancement, since the preceding is valid for a smooth tube.

When the condensate falls between the tubes, it will also have an obstructing effect on the vapour flow across the tube bank in the horizontal direction. This is modelled as an external body force, $F_{i'}$, in equation (2). The sign will be negative, since it is a momentum sink, and it will only exist for $i' = 1$, i.e. in the horizontal direction across the tube bank. It will only exist in narrow zones below the centre of each tube, where the condensate is assumed to flow. The further down the tube bank, the greater the magnitude of the momentum sink.

3.4 Condensation Heat Transfer

In order to further simplify the problem, the energy equation is not solved explicitly. Instead, saturated conditions are assumed in the entire condenser. This is a convenient simplification resulting in that the temperature can be calculated from composition and saturation data.

The starting point for heat transfer calculations is the over all heat flux equation:

$$dQ = UdA(T_I - T_c) \tag{8}$$

where dA is the area, T_I and T_c are interface temperature and temperature of the cooling water flowing inside the tube, respectively. U is the overall heat transfer coefficient, calculated from:

$$\frac{1}{UdA} = \frac{1}{h_i dA_i} + \frac{R_i}{dA_i} + \frac{\delta_w}{\lambda_w dA_w} + \frac{R_o}{dA_o} + \frac{1}{h_l dA_o} \tag{9}$$

where h_i is heat transfer coefficient on the inside of the tube, calculated from the Dittus-Boelter equation, R is fouling resistance, λ_w is thermal conductivity in the tube material and δ_w is tube thickness. h_l is the heat transfer coefficient in the condensate film, which is calculated according to the correlation for enhanced tubes by Beatty and Katz (1948):

$$h_l = 0.689\left(\frac{\lambda_l^3 \rho_l^2 g h_{fg}}{\mu_l (T_I - T_w) d_{eq}}\right)^{1/4} \tag{10}$$

where λ is the thermal conductivity, h_{fg} is the specific enthalpy of vapourization, T_I and T_W are temperatures at the phase interface and at the tube wall respectively, and d_{eq} is an equivalent diameter of the finned tube (Beatty and Katz 1948). According to Brown and Bansal (1999), this model sometimes underpredicts heat transfer for high fin densities, but Jung et al. (2003a) and Belgazi et al. (2001, 2003) have shown reasonably good agreement for several geometries. Here the relative difference between a pure fluid and a mixture is the main factor of importance, and this has not yet been thoroughly investigated. Recent experimental results by Honda et al. (1999, 2002) and Belghazi et al. (2001, 2003) show little effect of inundation for a mixture on a bundle of low-finned tubes, which means that the heat transfer coefficient is almost constant for the different tube rows, even though lower tube rows receive condensate

flow from the tubes above. Therefore, inundation effects are neglected in these calculations and equation (10) is used for all tubes without any adjustments.

For a mixture, the total heat flux calculated in equation (8) comes from three sources: cooling the vapour, cooling the condensate, and from condensation. The first two are consequences of the composition shift and the related change in saturation temperature. Investigations show that cooling the vapour generally stands for less than 4% of the total heat flux, and that term is therefore omitted here. Cooling the condensate, Q_{cc}, can be more important, especially on the lower tubes, and it is calculated from:

$$dQ_{cc} = \frac{dA_o}{A_o} \Gamma c_p \left(T_{sat-1} - T_{sat} \right) \tag{11}$$

where T_{sat-1} and T_{sat} are saturation temperatures on the tube above and on the actual tube respectively. For pure R22 dQ is solely the latent heat released by condensation, since the entire system is supposed to be saturated, and the pressure drop in a tube bank generally is low.

3.5 Condensation Mass Transfer

In order to solve equation (8) the interface temperature is needed, which depends on the interface composition. The interface composition is not straight-forward to calculate. Theoretical results by Sajjan et al. (2004) and Karlsson and Vamling (2004a) suggest that, especially for high heat fluxes, the mode of condensation is close to differential, meaning no mixing of newly formed condensate and condensate falling in from tubes above. This implies a high mass transfer resistance in the liquid phase, and with this assumption the composition of the condensing flux is the same as the liquid composition in equilibrium with the vapour closest to the interface. Thus the interface composition can be calculated from equilibrium data. Due to resistance to mass transfer in the vapour, a composition gradient will arise in the vapour close to the tube, so the vapour composition close to the interface will generally not be the same as in the vapour bulk.

In contrast to the differential mode of condensation, the integral mode of condensation means perfect mixing between newly formed condensate and condensate falling in from tubes above. Here the condensing flux, perfectly mixed with the incoming condensate from tubes above, will be in equilibrium with the vapour close to the tube. This will generally mean a more favourable interface composition, i.e. a higher interface temperature. Attaining interface equilibrium when assuming integral mode of condensation in the calculations has to be done by an iterative procedure. Both modes of condensation will be tested in the calculations presented here since there is no simple way to determine which mode of condensation occurs in a condenser, and since it is interesting to look at the extremes.

A diagram of the calculation algorithm for the external subroutines handling condensation is shown in Fig. 2 on next page. For every main iteration in the CFD program the algorithm is run through once for each location where condensation is supposed to occur, i.e. in all calculation cells adjacent to a tube. This means in the three-dimensional case many thousand times for each iteration.

There are two different paths for point 2 in the algorithm. The simpler one deals with the differential mode, shown in D1 in the figure. Here the composition of the condensing flux depends only on the vapour composition closest to the interface. For this a function is calculated in advance from equilibrium data, which states the composition of the condensing flux from a given vapour composition at the phase interface. From the composition of the condensing flux, the interface temperature can be calculated, since the condensate is supposed not to be mixed.

The integral version of the algorithm is more complex, which is seen to the right in Fig. 2. The top tubes in the bundle are still calculated as for the differential mode, mostly due to convergence issues. For the rest of the tubes, the composition of the condensing flux is calculated so that equilibrium is obtained at the interface. The composition in the vapour at the interface is read from the CFD program, and the

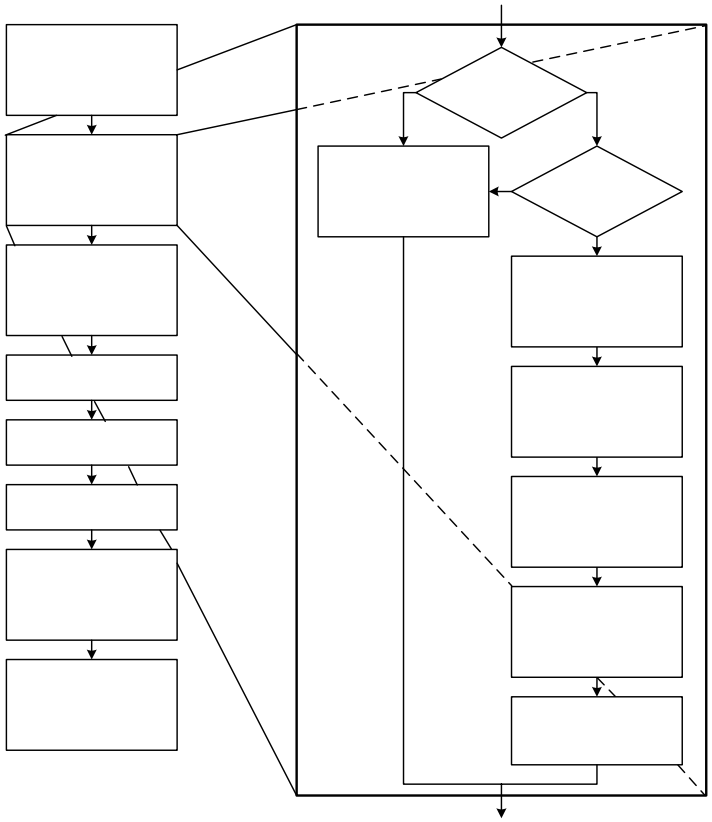

Fig. 2. Calculation algorithm used in the external subroutine.

liquid composition that fulfils the assumption of equilibrium between the phases is calculated from an equilibrium relation:

$$x_{eq} = f(y^*) \tag{12}$$

The bulk and interface composition of the liquid is the same since the condensate is assumed to be perfectly mixed. x_{eq} is the desired composition, which is controlled by the condensate flowing in from above and the condensing flux in a calculation cell. The inflow of condensate from above cannot be adjusted, but the composition of the condensing flux, x_{cond}, which fulfils the condition of equilibrium, can be calculated from a mass balance:

$$\frac{x_{inflow} \cdot N_{inflow} + x_{cond} \cdot N_{cond}}{N_{inflow} + N_{cond}} = x_{eq} \tag{13}$$

where x is composition and N is flux. Index *inflow* means condensate coming in from above, *cond* means condensing flux, and *eq* means in equilibrium with current vapour composition. Since N_{cond} is not yet calculated, it is taken from data stored in the previous iteration. The resulting value for x_{cond} is then weighed (in I5 in Fig. 2) with the result from the previous iteration according to:

$$x_{cond,use} = \frac{x_{cond} + 3 \cdot x_{cond,prev.iteration}}{4} \tag{14}$$

The reason is that the progress towards the solution will be smoother, and the number of iterations required to calculate the flow field and composition in the vapour bulk is large anyway. The calculations require several thousand iterations to converge. All thermophysical properties used in the calculation model are calculated locally from polynomial expressions, fitted to data from Refprop 7 (Lemmon et al. 2002).

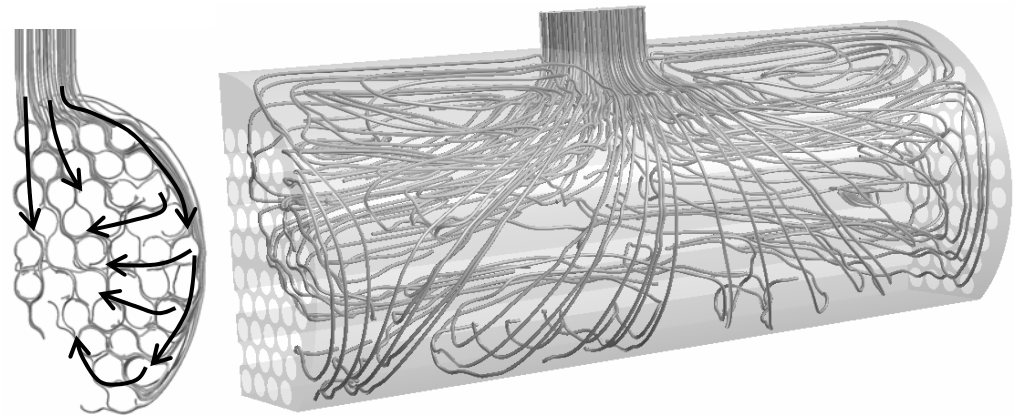

Fig. 3. Flow field for R22.

4 RESULTS AND DISCUSSION

The main focus of this work is to compare the flow fields for pure R22 and for the binary mixture. Calculations have been carried out as described above, which meant a couple of hours of calculation time for the case with R22, around a week calculation time for the differential mode with the mixture, and a couple of weeks calculation time for the integral mode with the mixture, all on a standard PC. The calculations took much longer for the mixture since a lot of variables had to be stored in order to handle the condensate, and the memory handling in the CFD program is limited and slow. The integral case needs to keep track of even more variables than the differential case (i.e. composition), hence the even longer calculation time.

It is difficult to present three-dimensional results in a good way. Here flow fields are presented as three-dimensional path lines, i.e. lines connecting vectors in the vapour flow field, creating a comprehensible image. Figure 3 is a description of the flow field for pure R22. Just as in the results from 2D calculations presented by Karlsson and Vamling (2004b), the vapour path is short and fairly straight. Some vapour hits the side walls, turns and flows back along the tubes, but otherwise the flow is as expected.

Figure 4 shows path lines for the mixture when assuming differential mode of condensation, i.e. no mixing in the condensate. The flow field is slightly different with a vortex forming in the lower part of the condenser. The flow field is more complex than for the pure fluid.

In Fig. 5 the same is shown when assuming integral mode of condensation, i.e. perfect mixing in the condensate. The vortex is even greater than in the previous figure. Vapour flows down along the shell and enters the tube bank from below causing counterflow between vapour and condensate. This is also similar to results from 2D calculations in previous work.

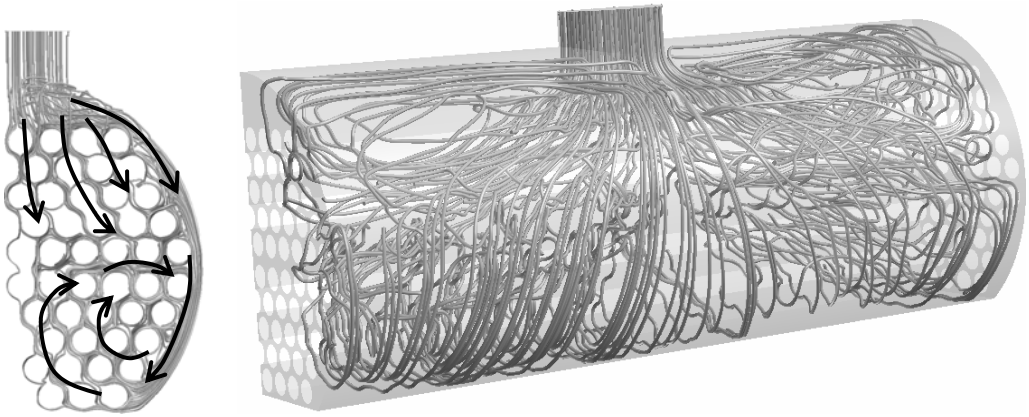

Fig. 4. Flow field for the mixture; differential mode.

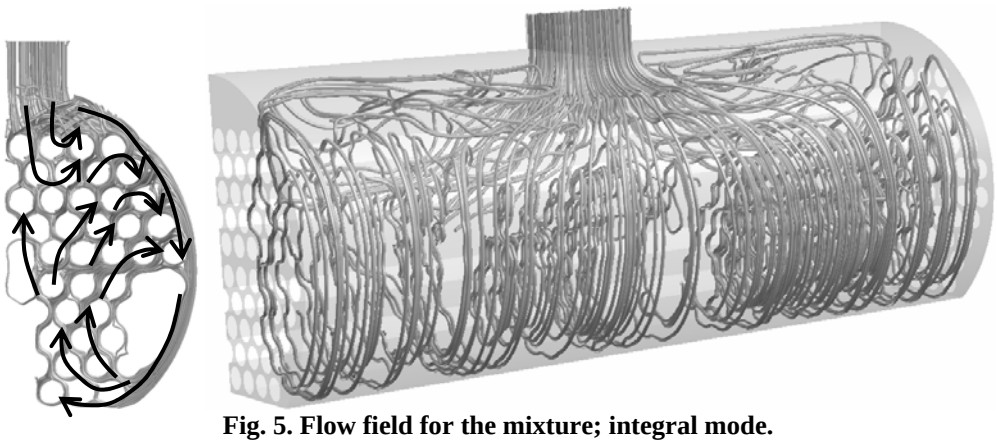

Fig. 5. Flow field for the mixture; integral mode.

Next, the composition of the mixture inside the condenser is presented as profiles along lines in six different locations depicted in Fig. 6. The composition profiles are seen in Fig. 7 for both modes of condensation. It can clearly be seen that the integral mode of condensation results in a higher mass fraction R32, which is the more volatile component of the two. Higher mass fraction R32 means a lower dew point temperature, hence a lower temperature driving force for heat transfer. Consequently the integral mode (to the right in Fig. 7) is inferior to the differential mode regarding heat transfer.

This result is surprising, since hand books always state that integral mode of condensation is superior to the differential mode. The reason is of course the complex flow field of the vapour. All standard calculation models assume: a) an even distribution from the inlet over all the tubes in the top row, and b) a well behaved vertical flow field from the top tube row down through the bundle. None of the two is true here. In Fig. 8 the total duty can be seen. It is around 41 kW when assuming no condensate mixing, but only 29 kW when assuming a well-mixed condensate, i.e. a 30 % lower duty.

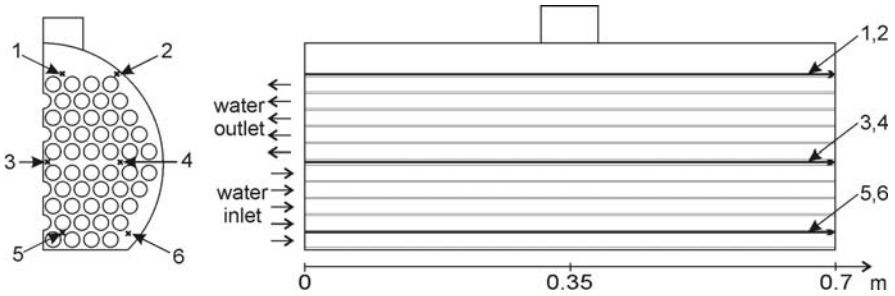

Fig. 6. Locations used for plots in Fig. 7.

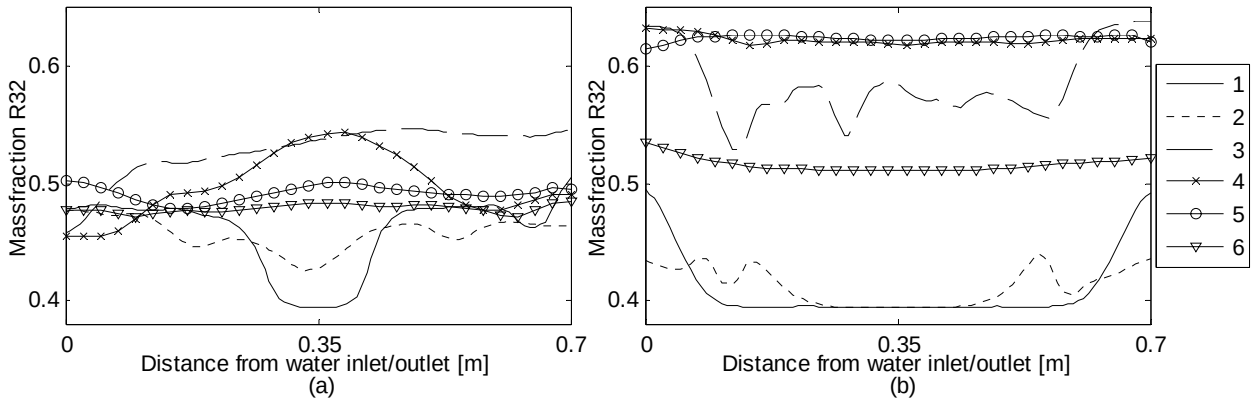

Fig. 7. Composition in condenser at different locations. (a) differential mode, (b) integral mode.

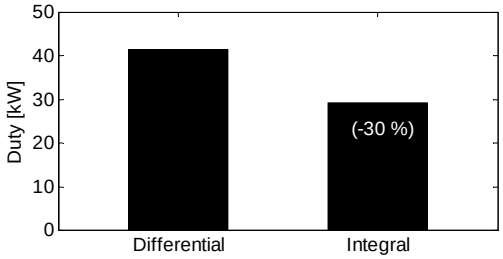

Fig. 8. Total condenser duty when condensing the mixture.

The results presented here is another piece in the puzzle of finding the reasons for performance drops when replacing pure refrigerants with mixtures. Earlier, mass transfer resistance in the vapour and in the condensate have been investigated (Sajjan et al. 2004 and Karlsson and Vamling 2004a). This work illustrates that the flow field is complex and may have an influence on the rate of heat transfer.

The next step in this investigation will be to try different inlet designs and in that way to see the magnitude of the influence of the flow field. This may be very important for future design of condensers for mixture condensation, and should be investigated in detail, not only theoretically, but also experimentally. Unfortunately, long calculation times did not allow a theoretical analysis of the inlet design to be included in the present work.

5 CONCLUSIONS

Advanced three-dimensional calculations have been carried out on condensation of pure R22 and a binary zeotropic refrigerant mixture on the shell-side of a horizontal shell-and-tube condenser. From the results and the discussion above the following conclusions can be drawn:

1. The calculated flow field for pure R22 is, as expected, presented by a relatively short and straight flow path.
2. The flow field for the mixture is more complex, with large vortexes forming in the lower part of the condenser, more distinct for the integral mode than for the differential mode of condensation.
3. The vortex causes the vapour to enter the tube bundle from the bottom, causing a counterflow between vapour and condensate.
4. The counterflow causes unfavourable interface composition and therefore poor heat transfer.
5. For the conditions studied here, the flow field for the integral mode of condensation results in a 30 % lower heat flux compared to the differential mode under equal conditions. This is in contrast to all standard theories which state the opposite relation.
6. Results show that standard calculation models for mixture condensation may be misleading due to simplifications of the flow field.

REFERENCES

Beatty K.O. and D.L. Katz 1948. “Condensation of vapors on the outside of finned tubes,” *Chem Eng Prog*, Vol. 44, pp. 55-70.

Belghazi M., A. Bontemps, J.C. Signe, and C. Marvillet 2001. “Condensation heat transfer of a pure fluid and binary mixture outside a bundle of smooth horizontal tubes. Comparison of experimental results and a classical model,” *Int J Refrigeration* Vol. 24, pp. 841-855.

Belghazi M., A. Bontemps, and C. Marvillet 2003. “Experimental study and modeling of heat transfer during condensation of pure fluid and binary mixture on a bundle of horizontal finned tubes,” *Int J Refrigeration*, Vol. 26 pp. 214-223.

Bird R.B., W.E. Stewart, and E.N. Lightfoot 2001. *Transport phenomena*. John Wiley and Sons Ltd, 2nd edition, New York, USA.

Brown M.W. and P.K. Bansal 1999. "An overview of condensation heat transfer on horizontal tube bundles," *Applied Thermal Eng*, Vol. 19, pp. 565-594.

Fuller E.N., Ensley K., and J.C. Giddings 1969. "Diffusion of halogenated hydrocarbons in helium. The Effect of structure on collision cross sections," *J Phys Chem*, Vol. 73, pp. 3679-3685.

Fuller E.N., P.D. Schettler, and J.C Giddings 1966. "A new method for prediction of binary gas-phase diffusion coefficients," Ind and Eng Chem Vol. 58, pp. 19-27.

Gabrielii C. and L. Vamling 1997. "Replacement of R22 in tube-and-shell condensers: experiments and simulations," *Int J Refrigeration*, Vol. 20, pp. 165-178.

Honda H., H. Takamatsu, and N. Takata 1999. "Experimental measurements for condensation of downward-flowing R123/R134a in a staggered bundle of horizontal low-finned tubes with four geometries," *Int J Refrigeration*, Vol. 22, pp. 615-624.

Honda H., H. Takamatsu, and N. Takata 2002. "Condensation of downward-flowing zeotropic mixture HCFC-123/HFC-134a on a staggered bundle of horizontal low-finned tubes," *Int J Refrigeration*, Vol. 25, pp. 3-10.

Jung D., C. Kim, S. Hwang, and K. Kim 2003a. "Condensation heat transfer coefficients of R22, R407C, and R410A on a horizontal plain, low fin, and turbo-C tubes," *Int J Refrigeration*, Vol. 26, pp. 485-491.

Jung D., K. Song, K. Kim, and K. An 2003b. "Condensation heat transfer coefficients of halogenated binary refrigerant mixtures on a smooth tube," *Int J Refrigeration*, Vol. 26, pp. 795-799.

Karlsson T. and L. Vamling 2004a. "Reasons for drop in shell-and-tube condenser performance when replacing R22 with zeotropic mixtures – Part 2: Investigation of mass transfer resistance effects," *Int J Refrigeration*, Vol. 27, pp. 561-566.

Karlsson T. and L. Vamling 2004b. "Consequences of flow field on mixture condensation in a shell-and-tube condenser," *Int J Refrigeration*, accepted for publication.

Lemmon E.W., M.O. McLinden, and M.L. Huber 2002. NIST Standard Reference Database 23 (Refprop), version 7.0, Physical and Chemical Properties Division, National Institute of Standards and Technology.

Liu J., H. Aizawa, and H. Yoshino 2004. "CFD prediction of surface condensation on walls and its experimental validation," *Building and Environment*, Vol. 39, pp. 905-911.

Nusselt W. 1916. "Die Oberflächenkondensation des Wasserdampfes," *VDI Zeitung*, Vol. 60, pp. 541-546, pp. 569-575.

Perrotin T. and D. Clodic 2004. "Thermal-hydraulic CFD study in louvred fin-and-flat-tube heat exchangers," *Int J Refrigeration*, Vol. 27, pp.422-432.

Sajjan D., T. Karlsson, and L. Vamling L 2004. "Reasons for drop in shell-and-tube condenser performance when replacing R22 with zeotropic mixtures – Part 1: Analysis of experimental findings," *Int J Refrigeration*, Vol. 27, pp. 552-560.

UN 1989. "Montreal protocol on substances that deplete the ozone layer," *United Nations Environment Programme*, Final Act.